Unveiling the Higgs at FCC-hh

With new diboson precision measurements

Pheno 2021

26 May 2021

Alejo N. Rossia

DESY Hamburg Theory Group

Institut für Physik, Humboldt-Universität zu Berlin

In collaboration with F. Bishara, P. Englert, C. Grojean, M. Montull, G. Panico

arXiv 2004.06122 (JHEP 07 (2020) 075)

arXiv 2011.13941 (JHEP 04 (2021) 154) (+ S. De Curtis, L. Delle Rose)

Motivation

- **We need Physics Beyond the Standard Model**
- **Precision with hadron colliders? Yes!**

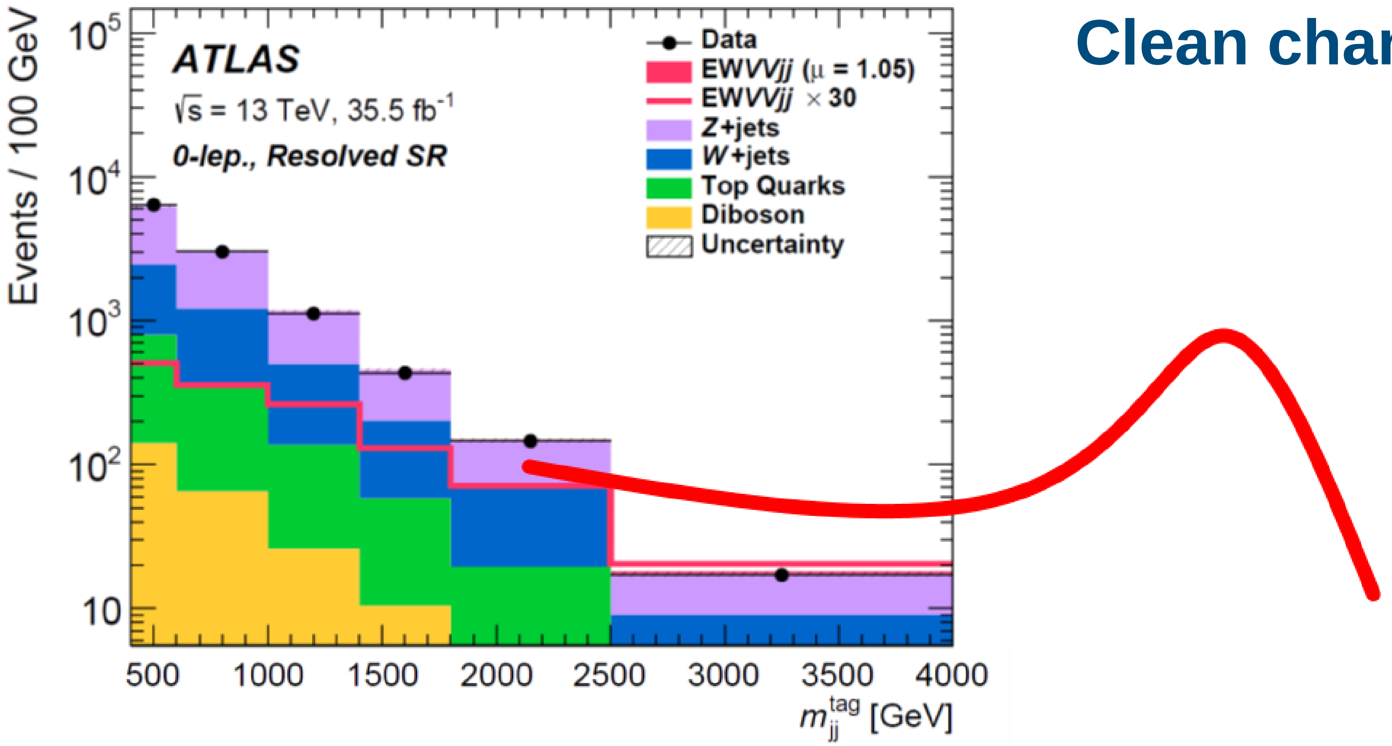

ATLAS, 1905.07714

Clean channels + NP effects that grow with E

↓

Tail hunting!

Heavy New Physics

↓

Effective Field Theories

Diboson processes are useful

Leptonic diphoton Wh.

arXiv 2004.06122 (JHEP 07 (2020) 075)

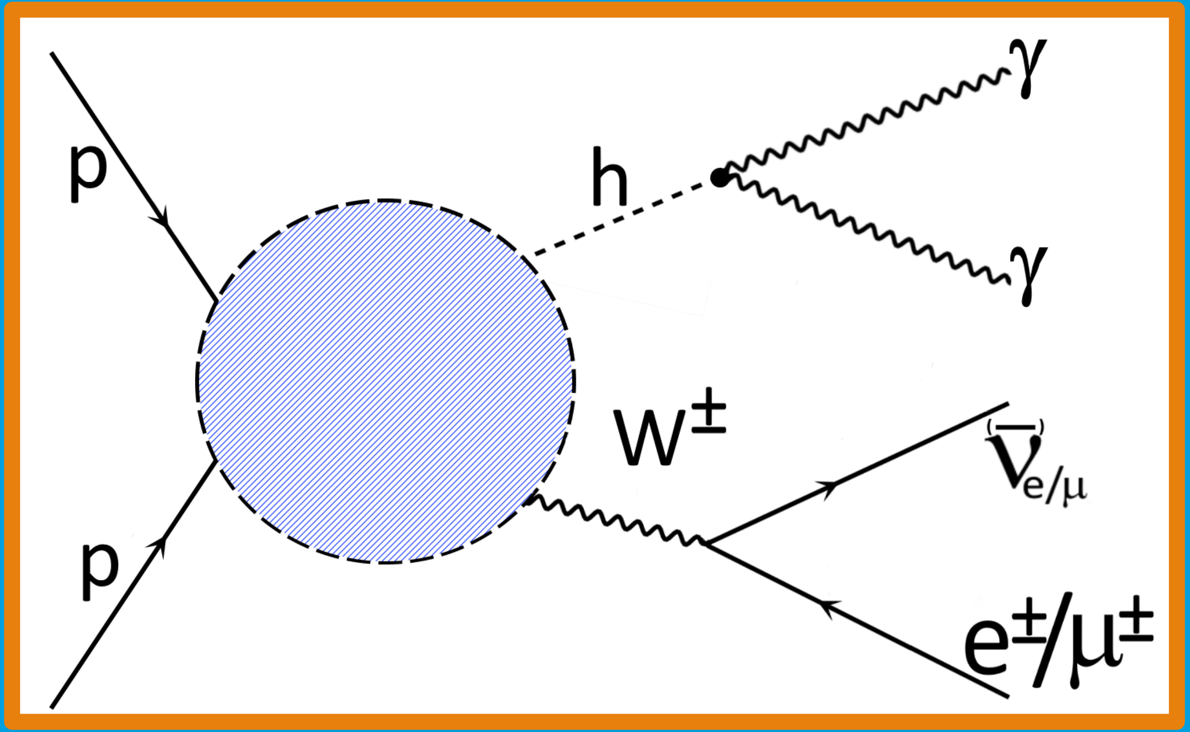

$$pp \to W^{\pm} h \to l^{\pm} \nu \, \gamma\gamma$$

What New Physics can we probe?

- Assumptions: SMEFT + Dim. 6 op. in Warsaw basis + MFV.

High energy behavior

$$\frac{c_{\varphi q}^{(3)}}{\Lambda^2}\left(\overline{Q}_L \sigma^a \gamma^\mu Q_L\right)\left(i H^\dagger \sigma^a \overleftrightarrow{D}_\mu H\right) \longrightarrow \frac{\mathcal{A}_{BSM}}{\mathcal{A}_{SM}} \sim \hat{s}$$

$$\left.\begin{aligned} &\frac{c_{\varphi W}}{\Lambda^2} H^\dagger H\, W^{a,\mu\nu} W^a_{\mu\nu} \\ &\frac{c_{\varphi \widetilde{W}}}{\Lambda^2} H^\dagger H\, W^{a,\mu\nu} \widetilde{W}^a_{\mu\nu} \end{aligned}\right\} \longrightarrow \frac{\mathcal{A}_{BSM}}{\mathcal{A}_{SM}} \sim \sqrt{\hat{s}}$$

$$\widetilde{W}^{a,\mu\nu} \equiv \frac{1}{2}\epsilon^{\mu\nu\rho\sigma} W^a_{\rho\sigma}$$

Interference patterns

Measuring angles resurrects interference

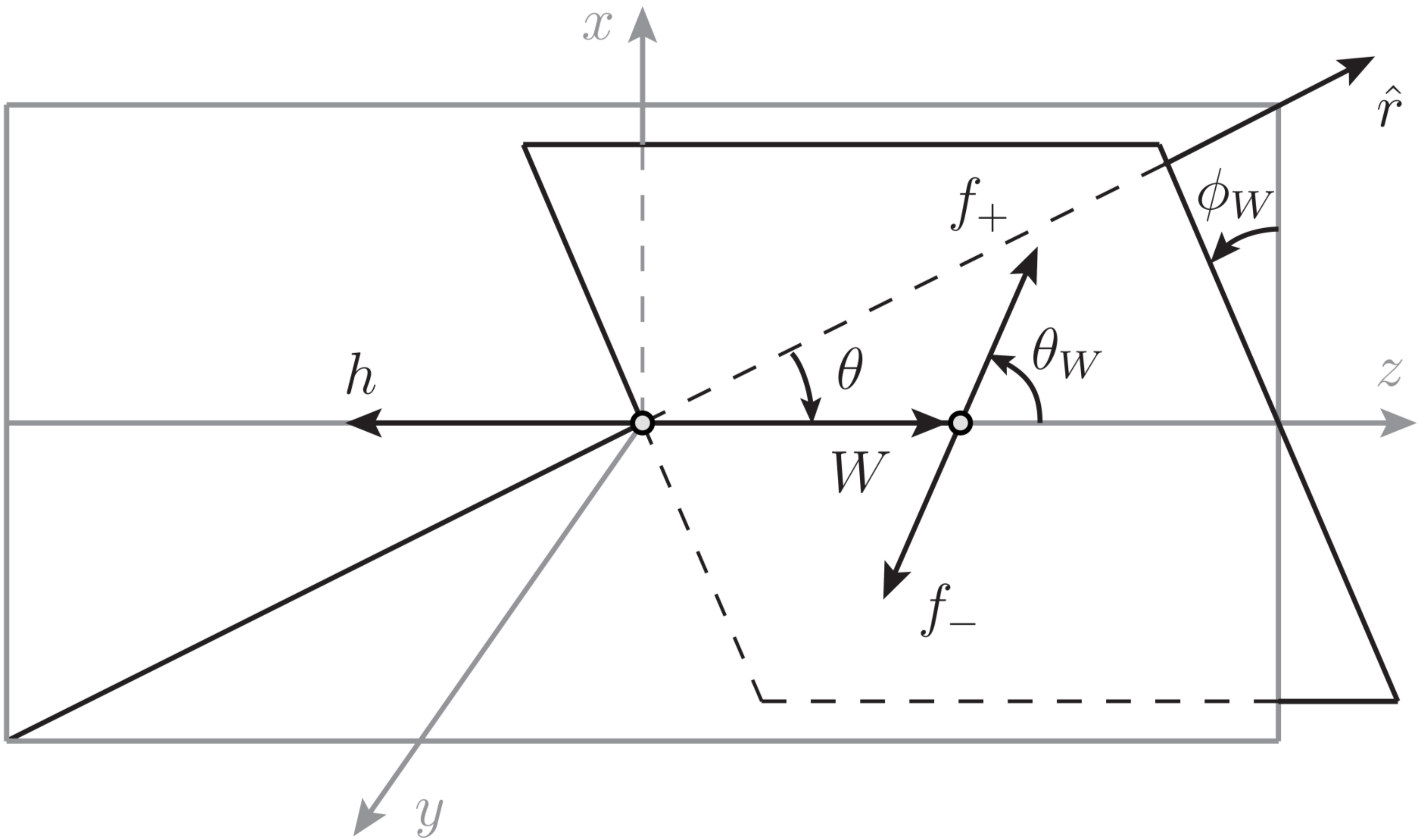

Interference patterns

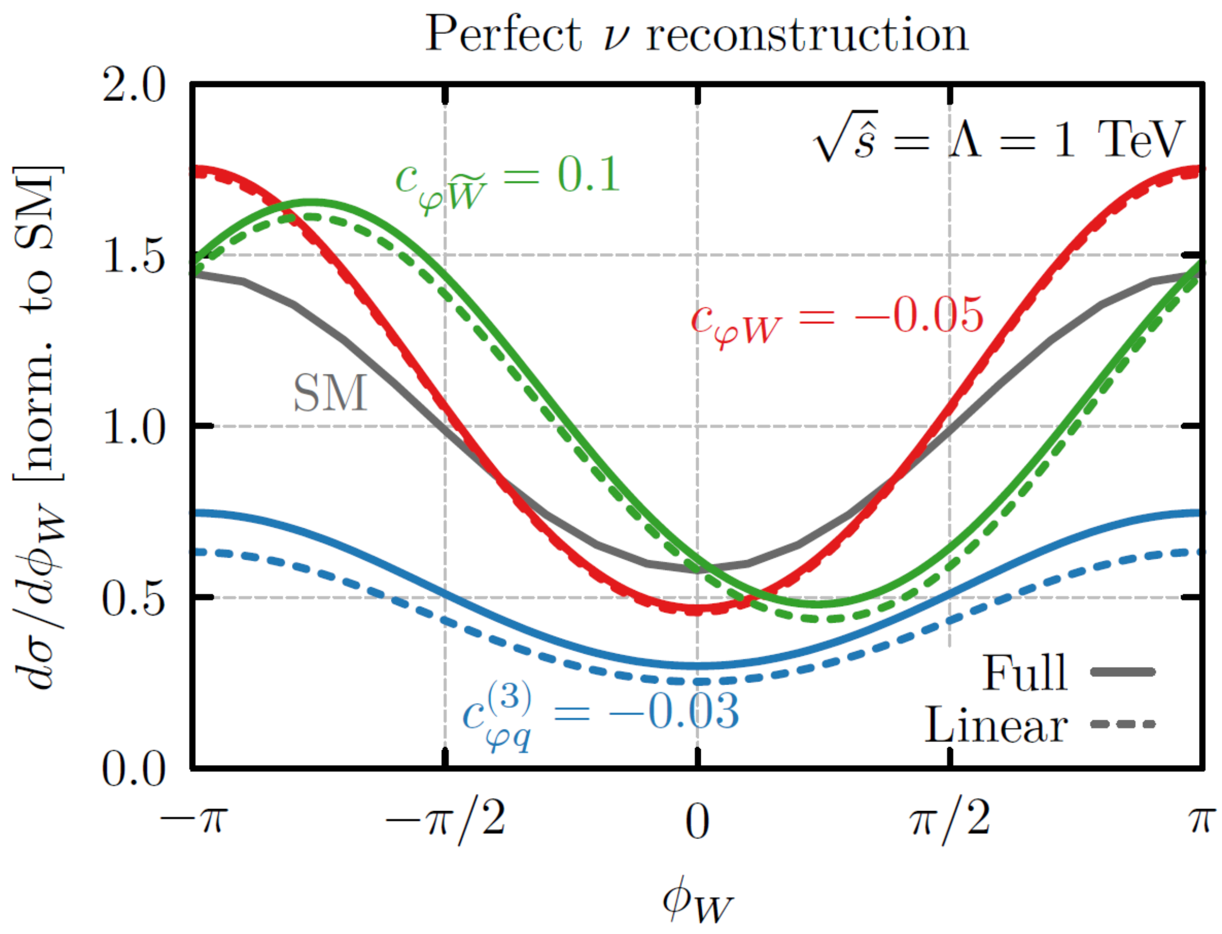

Differential in p_T^h and ϕ_W

$$\sigma^{int}_{\mathcal{O}^{(3)}_{\varphi q}} \sim \frac{\hat{s}}{\Lambda^2}$$

$$\sigma^{int}_{\mathcal{O}_{\varphi W}} \sim \frac{\sqrt{\hat{s}} M_W}{\Lambda^2} \cos(\phi_W)$$

$$\sigma^{int}_{\mathcal{O}_{\varphi \widetilde{W}}} \sim \frac{\sqrt{\hat{s}} M_W}{\Lambda^2} \sin(\phi_W)$$

$$p_T^h \in \{200, 400, 600, 800, 1000, \infty\}\ \text{GeV} \qquad \phi_W \in [-\pi, 0],\ [0, \pi]$$

Interference patterns

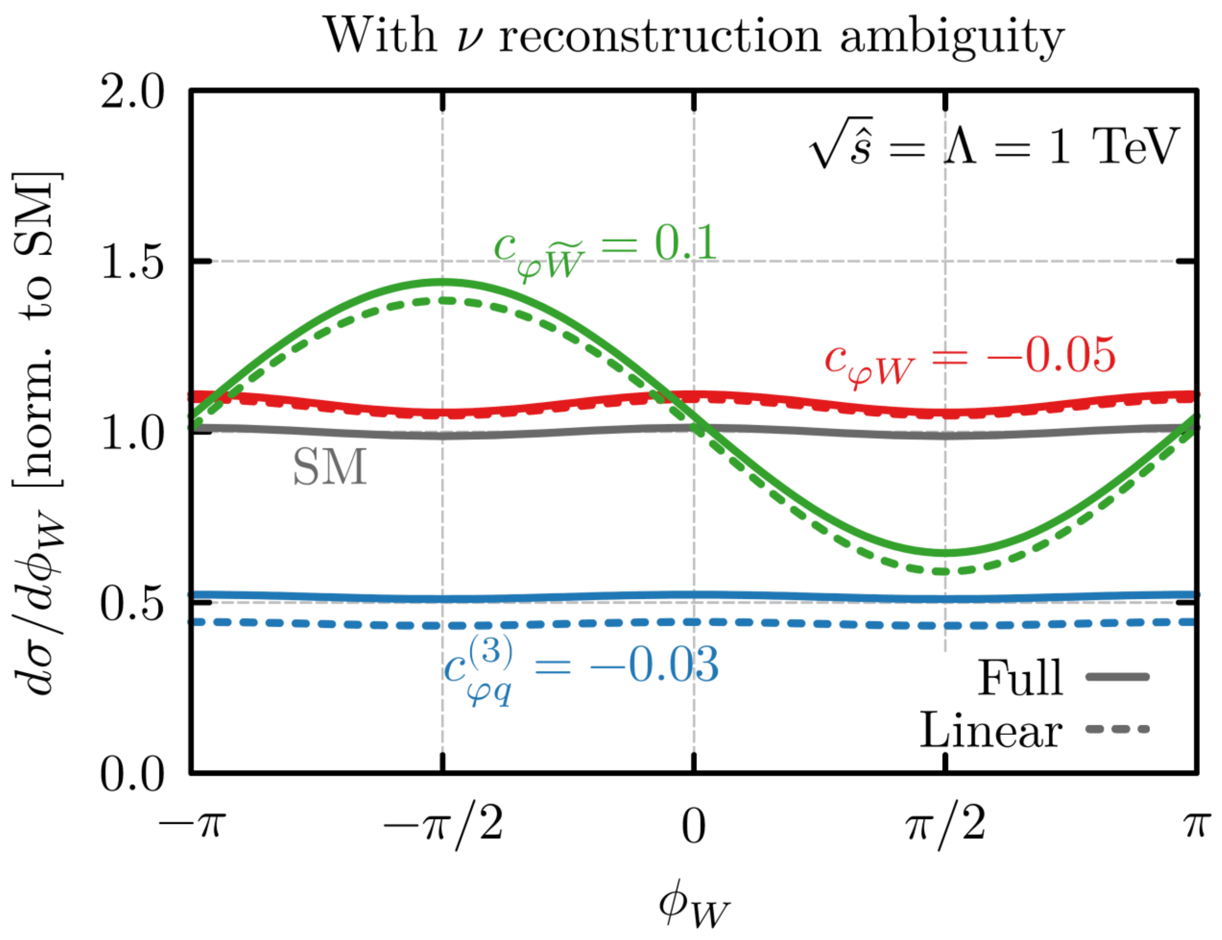

Differential in p_T^h and ϕ_W

$$\sigma^{int}_{\mathcal{O}^{(3)}_{\varphi q}} \sim \frac{\hat{s}}{\Lambda^2}$$

ν reconstruction ($\phi_W \to \pi - \phi_W$)

$$\sigma^{int}_{\mathcal{O}_{\varphi W}} \sim \frac{\sqrt{\hat{s}} M_W}{\Lambda^2} \cos(\phi_W)$$

$$\sigma^{int}_{\mathcal{O}_{\varphi \widetilde{W}}} \sim \frac{\sqrt{\hat{s}} M_W}{\Lambda^2} \sin(\phi_W)$$

$$p_T^h \in \{200, 400, 600, 800, 1000, \infty\}\ \text{GeV} \qquad \phi_W \in [-\pi, 0],\ [0, \pi]$$

Diphoton Zh.

arXiv 2011.13941 (JHEP 04 (2021) 154)

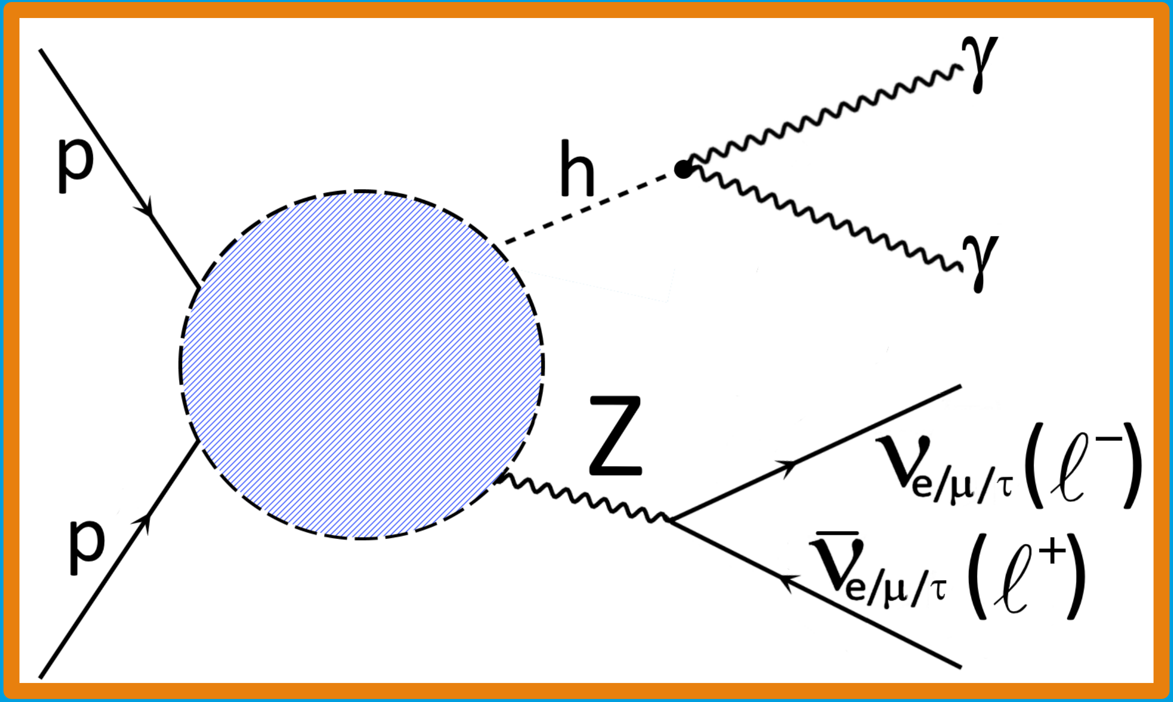

$$pp \to Zh \to l^+l^- \; (\nu\bar{\nu})\, \gamma\gamma$$

What New Physics can we probe?

- Assumptions: SMEFT + Dim. 6 op. in Warsaw basis + Flav. Univ.

High energy behavior

$$\frac{c_{\varphi q}^{(3)}}{\Lambda^2}\left(\overline{Q}_L\sigma^a\gamma^\mu Q_L\right)\left(iH^\dagger\sigma^a\overleftrightarrow{D}_\mu H\right)$$

$$\frac{c_{\varphi q}^{(1)}}{\Lambda^2}\left(\overline{Q}_L\gamma^\mu Q_L\right)\left(iH^\dagger\overleftrightarrow{D}_\mu H\right)$$

$$\frac{c_{\varphi u}}{\Lambda^2}\left(\overline{u}_R\gamma^\mu u_R\right)\left(iH^\dagger\overleftrightarrow{D}_\mu H\right)$$

$$\frac{c_{\varphi d}}{\Lambda^2}\left(\overline{d}_R\gamma^\mu d_R\right)\left(iH^\dagger\overleftrightarrow{D}_\mu H\right)$$

→

$$\frac{\mathcal{A}_{BSM}}{\mathcal{A}_{SM}}\sim\hat{s}$$

Interference patterns

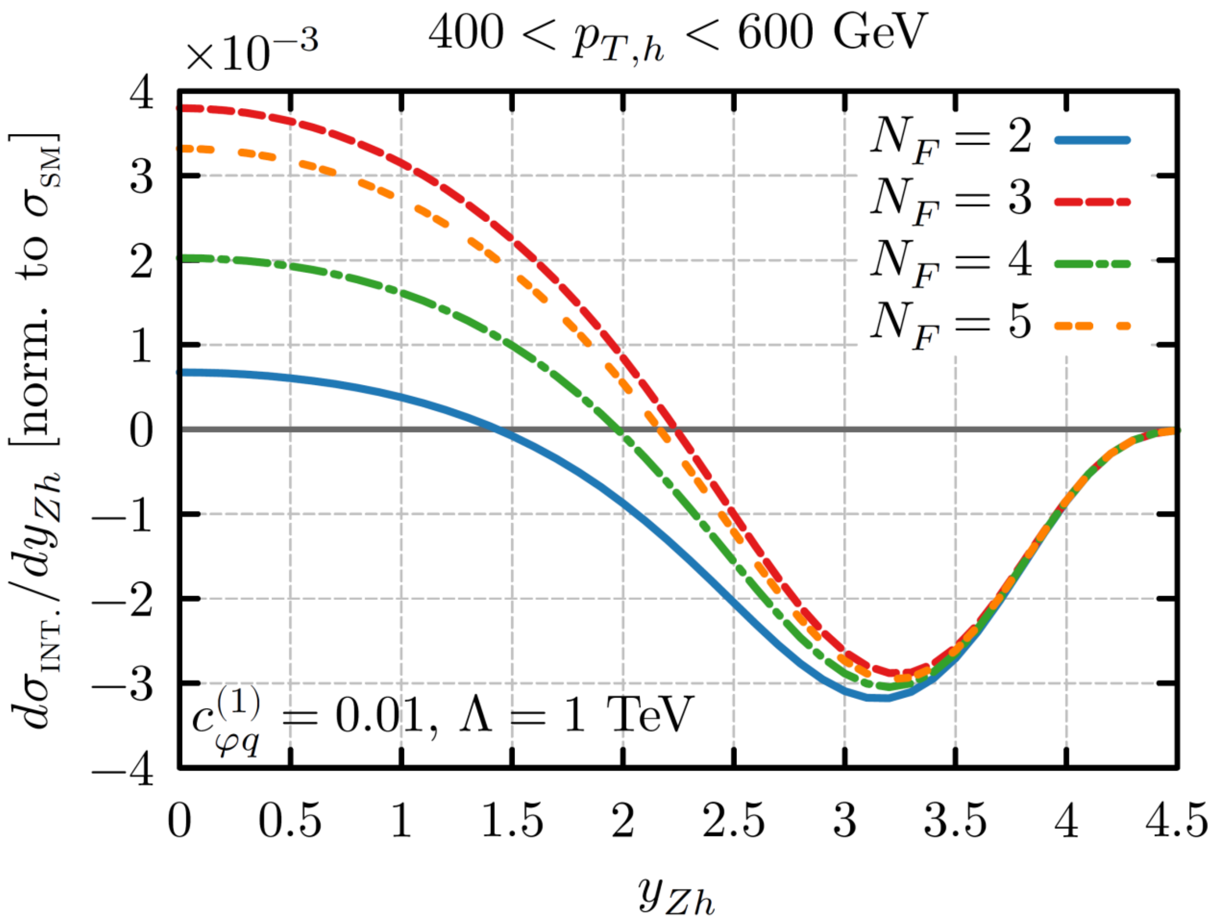

$$\sigma^{int}_{\mathcal{O}^{(1)}_{\varphi q}} \propto s_W^2 Q - T_3$$

Cancellation of up and down contributions

$$\sigma^{int}_{\mathcal{O}_{\varphi u(d)}} \propto g_R^{Zu(d)}$$

Suppression by SM coupling

Differential in p_T and rapidity

$$\mathrm{Min}\{p_T^h, p_T^Z\} \in \{200, 400, 600, 800, 1000, \infty\}\ \mathrm{GeV} \qquad |y_{Zh}| \in [0,2),\ [2,6]$$

(Slightly different rapidity binning for $Z \to \nu\bar{\nu}$)

Very competitive bounds for $c_{\varphi q}^{(3)}$ (*Zh* + *Wh* comb.)

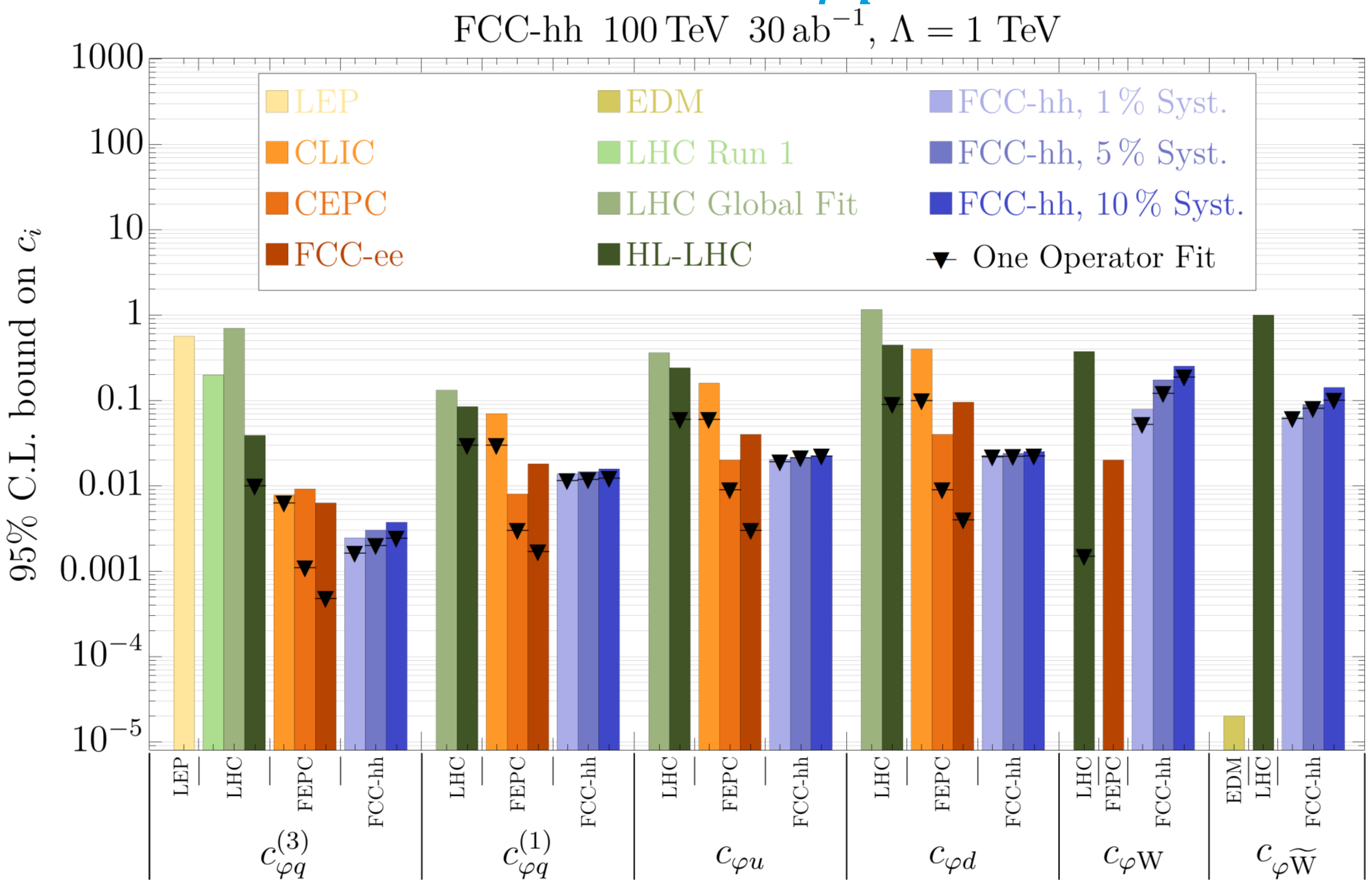

Sizeable impact on aTGC bounds

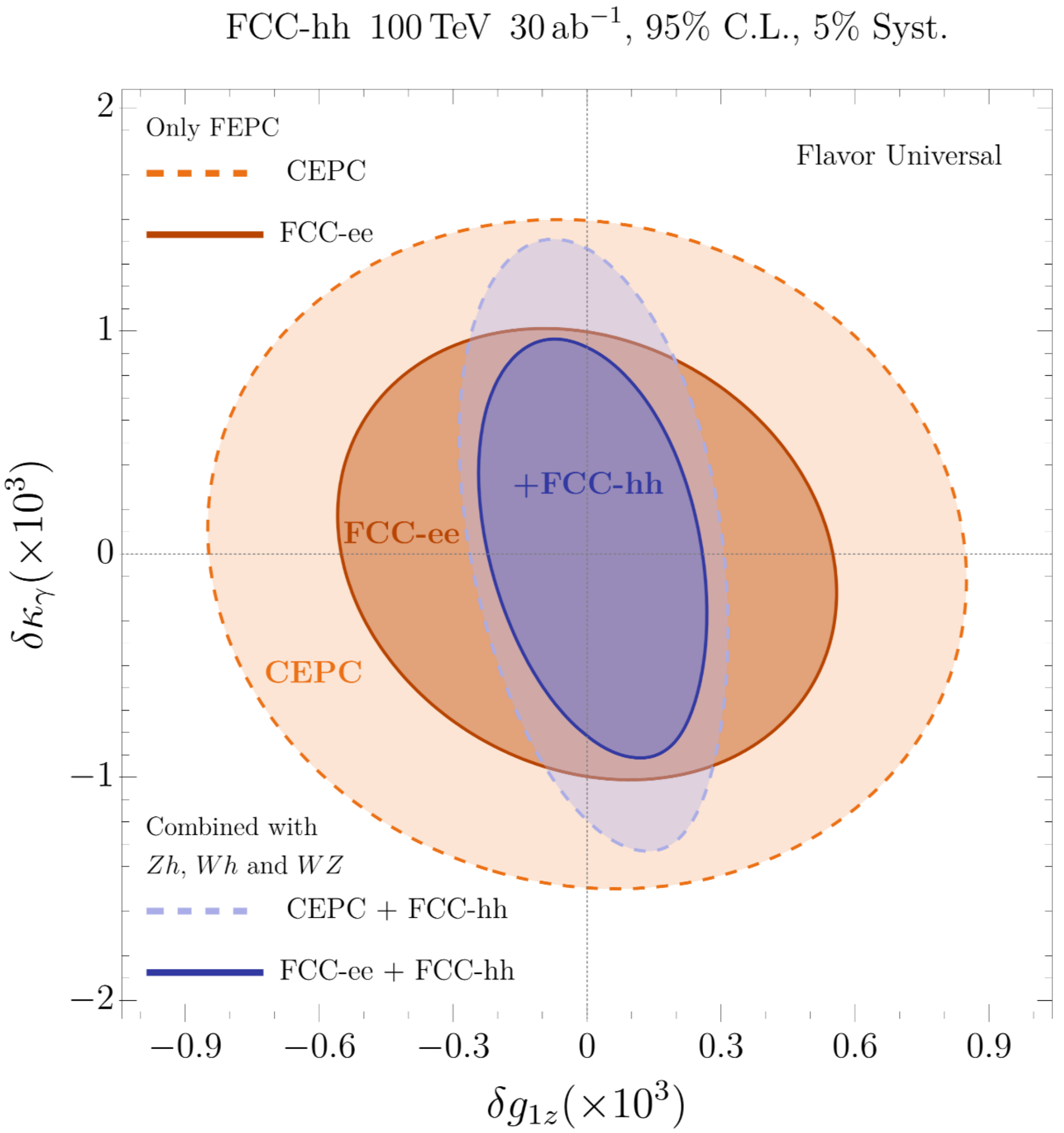

Conclusions

- New diboson channels to do precision measurements at FCC-hh, like Wh and Zh with $h \to \gamma\gamma$.
- With a simple p_T binning, they offer competitive sensitivity to $\mathcal{O}_{\varphi q}^{(3)}$.
- In Wh , a binning in ϕ_W gives an observable linear in $\mathcal{O}_{\varphi\widetilde{W}}$ with competitive sensitivity.
- In Zh, a binning in rapidity helps to overcome cancellations between different flavor contributions in $\mathcal{O}_{\varphi q}^{(1)}$.
- Wh and Zh with $h \to \gamma\gamma$ are not exploration channels, but important to probe different directions.

Thank you for your attention

Contact

DESY. Deutsches Elektronen-Synchrotron

www.desy.de

Alejo N. Rossia
DESY Theory Group
E-mail: alejo.rossia at desy dot de
https://theory-hamburg.desy.de/

Appendix.

For even more details, read our papers.

Wh.

Interference patterns

Helicity amplitudes: High energy behavior

W polarization	SM	$\mathcal{O}_{\varphi q}^{(3)}$	$\mathcal{O}_{\varphi \mathrm{W}}$	$\mathcal{O}_{\varphi \widetilde{\mathrm{W}}}$
$\lambda = 0$	1	$\frac{\hat{s}}{\Lambda^2}$	$\frac{M_W^2}{\Lambda^2}$	0
$\lambda = \pm$	$\frac{M_W}{\sqrt{\hat{s}}}$	$\frac{\sqrt{\hat{s}}\, M_W}{\Lambda^2}$	$\frac{\sqrt{\hat{s}}\, M_W}{\Lambda^2}$	$\frac{\sqrt{\hat{s}}\, M_W}{\Lambda^2}$

Wh.

Signal

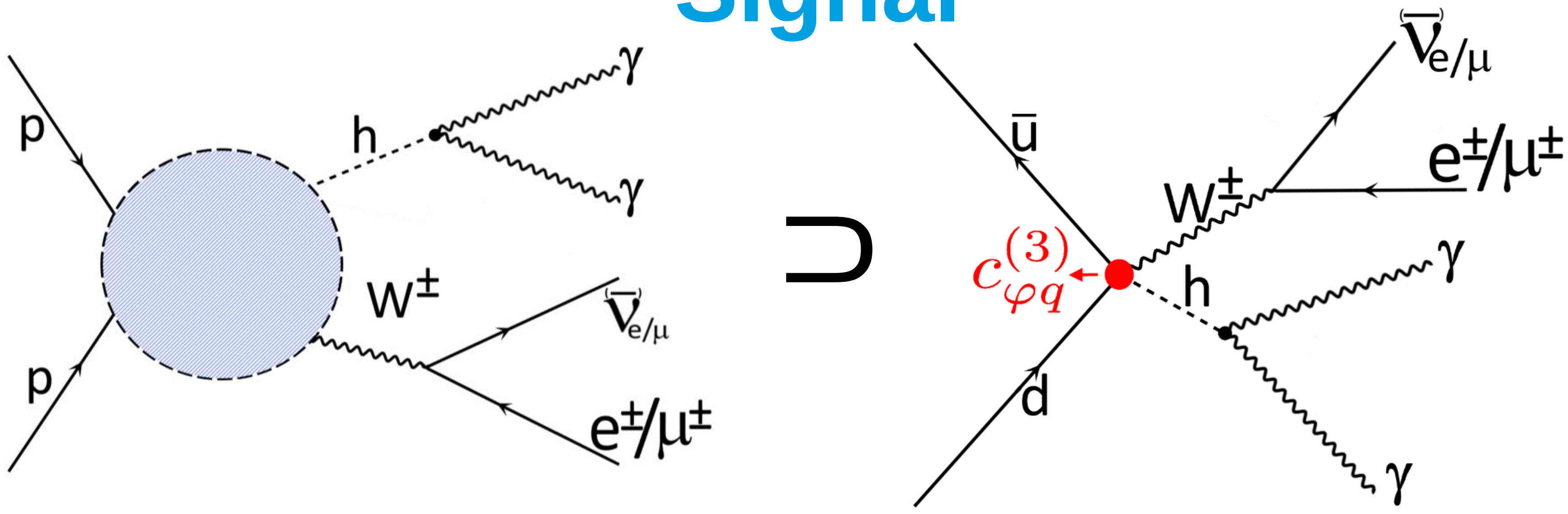

Background

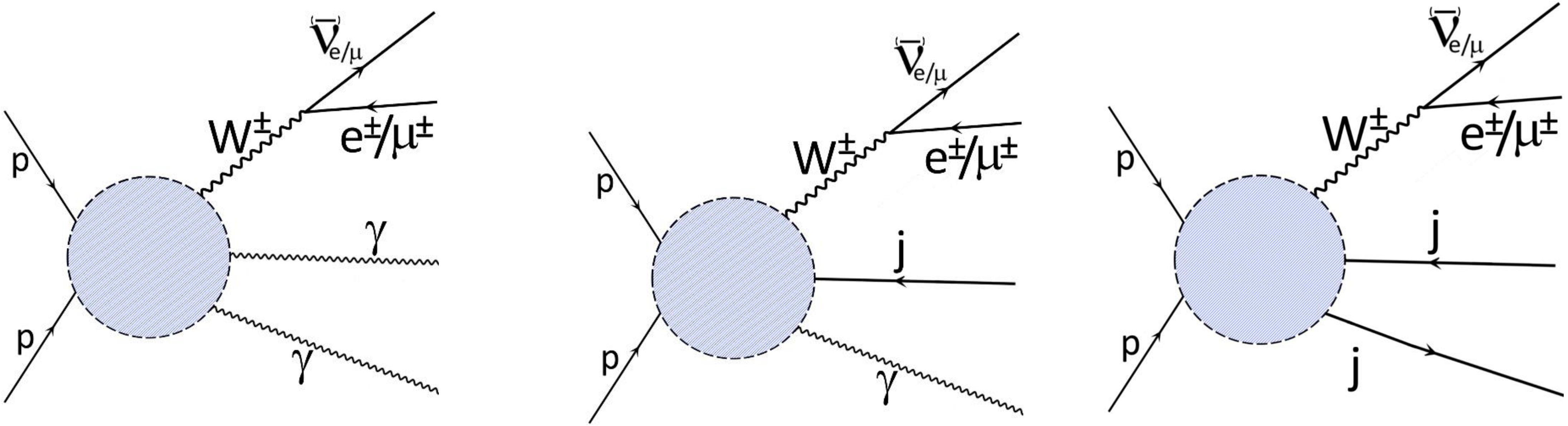

Wh.

Simulation details

- Montecarlo generation: Madgraph5_aMC@NLO v.2.6.5; showering: Pythia 8.2; detector simulation: Delphes v.3.4.1 with FCC-hh card.
- Signal and $W\gamma\gamma$ simulated at FO, the rest simulated at LO. QED k-factor for the signal.
- Parton level generation cuts:

	Wh	$W\gamma\gamma$	$Wj\gamma$ and Wjj
$p_{T,\min}^{\ell}$ [GeV]	30 (all samples)		
$p_{T,\min}^{\gamma,j}$ [GeV]	50 (all samples)		
$\not{E}_{T,\min}$ [GeV]	100 (all samples)		
$\lvert\eta_{\max}^{j,\ell}\rvert$	6.1 (all samples)		
$\Delta R_{\min}^{\gamma\gamma,\gamma j,\gamma\ell}$	–	0.01	0.01
$\Delta R_{\max}^{\gamma\gamma,\gamma j,jj}$	–	2.5	2
$m^{\gamma\gamma,\gamma j,jj}$ [GeV]	–	[50,300]	[50,250]
$p_{T,\min}^{h,\gamma\gamma}$ [GeV]	{150,350,550,750}	{100,300,500,700}	–
$p_{T,\min}^{\ell\nu}$ [GeV]	–	–	{100,300,500,700}

Wh. Analysis details

- Selection cuts and cutflow in the third p_T^h bin:

	Selection cuts
$p^{\ell}_{T,\text{min}}$ [GeV]	30
$p^{\gamma}_{T,\text{min}}$ [GeV]	50
$\not{E}_{T,\text{min}}$ [GeV]	100
$m_{\gamma\gamma}$ [GeV]	[120, 130]
$\Delta R^{\gamma\gamma}_{\text{max}}$	$\{1.3, 0.9, 0.75, 0.6, 0.6\}$
$p^{Wh}_{T,\text{max}}$ [GeV]	$\{300, 500, 700, 900, 900\}$

Selection cuts / efficiency	$\xi^{(3)}_{h\to\gamma\gamma}$	$\xi^{(3)}_{\gamma\gamma}$	$\xi^{(3)}_{j\gamma}$	$\xi^{(3)}_{jj}$
$\geq 1\ell^{\pm}$ with $p_T > 30$ GeV	0.86	0.46	0.94	0.94
$\geq 2\gamma$ each with $p_T > 50$ GeV	0.50	0.18	$5.7 \cdot 10^{-3}$	$8.7 \cdot 10^{-7}$
$\not{E}_T > 100$ GeV	0.49	0.16	$5.1 \cdot 10^{-3}$	$8.5 \cdot 10^{-7}$
120 GeV $< m_{\gamma\gamma} <$ 130 GeV	0.46	$6 \cdot 10^{-3}$	$2 \cdot 10^{-4}$	$8.2 \cdot 10^{-8}$
$\Delta R^{\gamma\gamma} < \Delta R_{max}$	0.45	$4 \cdot 10^{-3}$	$3.1 \cdot 10^{-5}$	$6.4 \cdot 10^{-8}$
$p_T^{Wh} < p^{Wh}_{T,max}$	0.41	$7 \cdot 10^{-4}$	$1.1 \cdot 10^{-5}$	$4.7 \cdot 10^{-8}$

Wh. More results

- Events per bin for the relevant processes

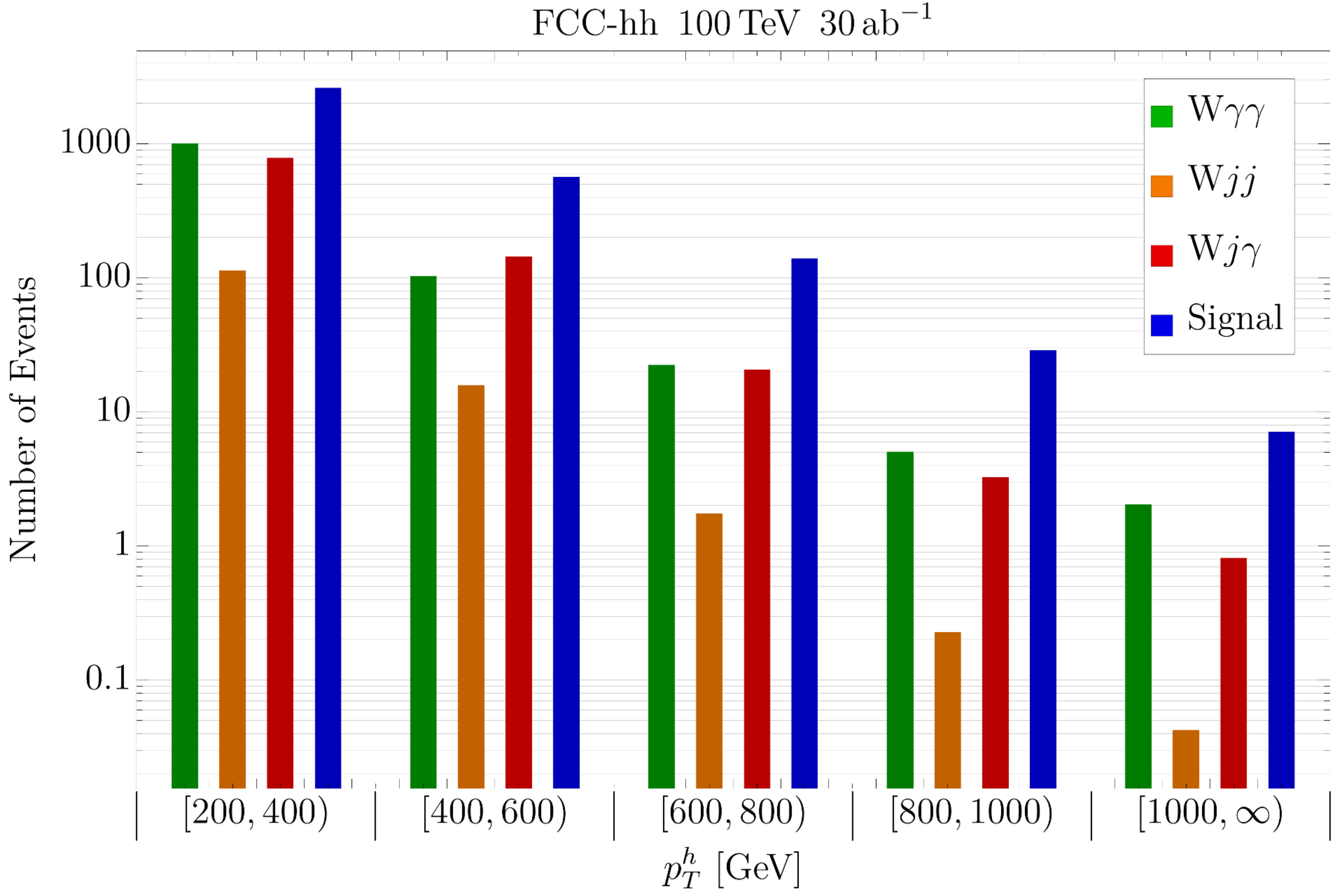

More results

- Bounds on $\mathcal{O}_{\varphi q}^{(3)}$ with one operator fit as a function of the NP scale M. See details in JHEP 07 (2020) 075, Fig. 5

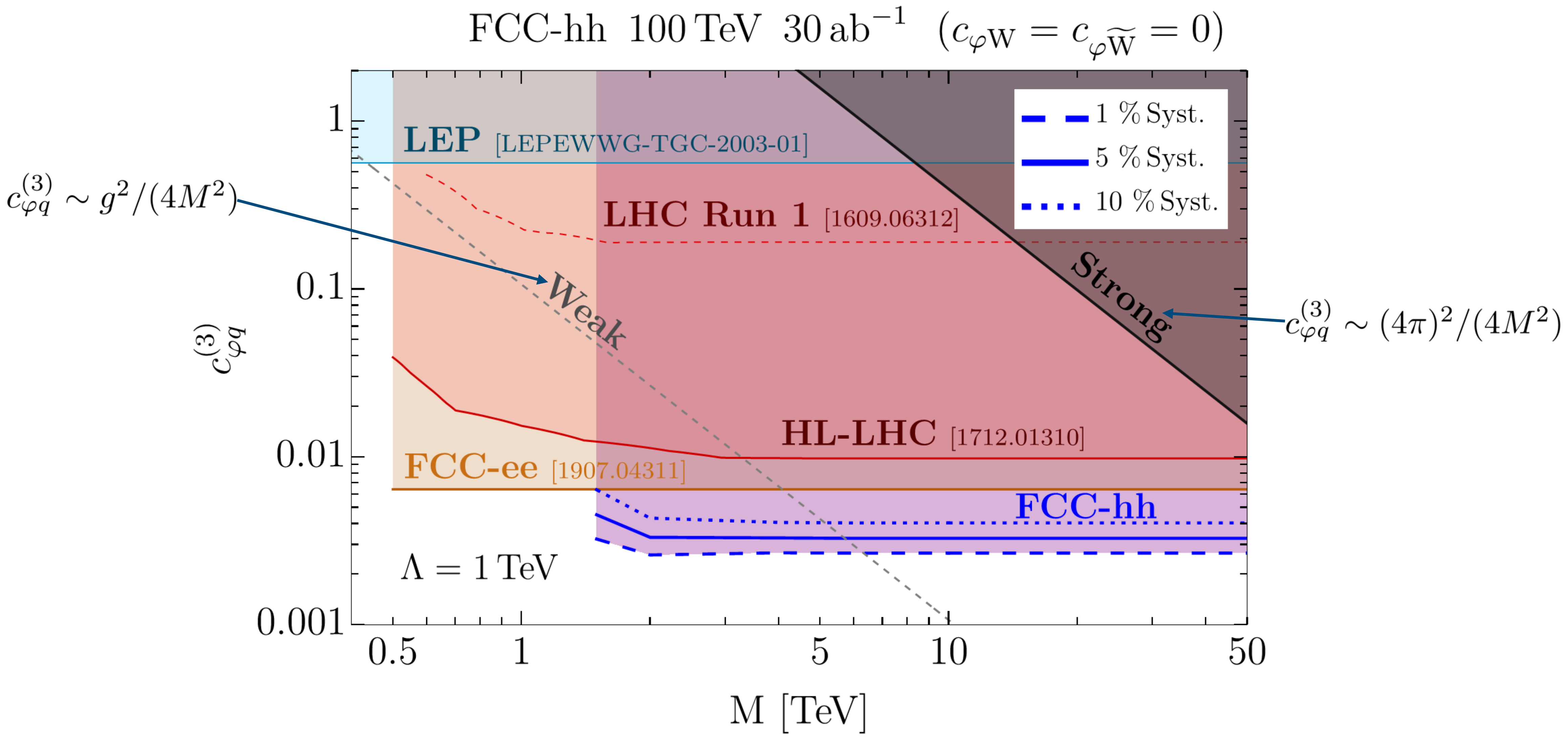

More results

- 95% CL bounds

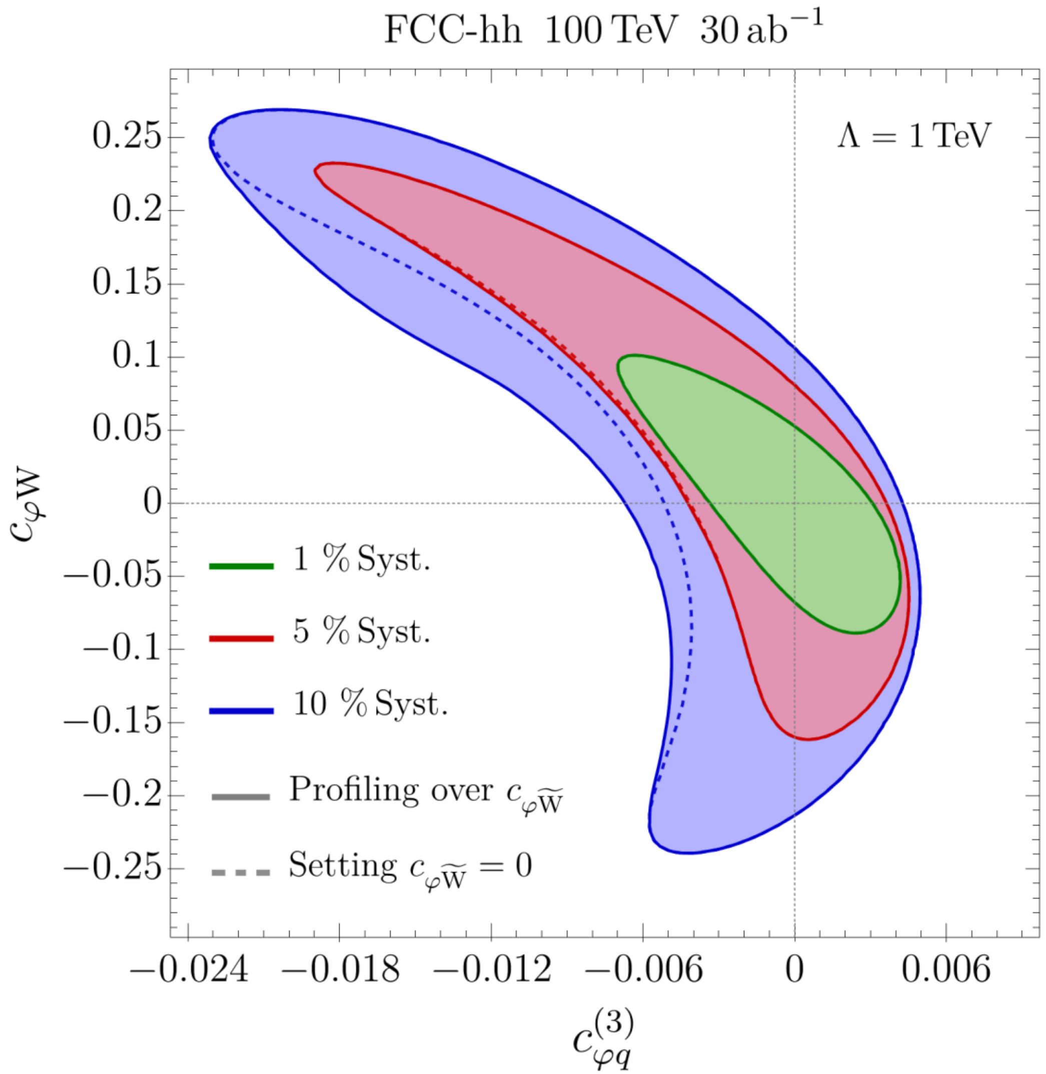

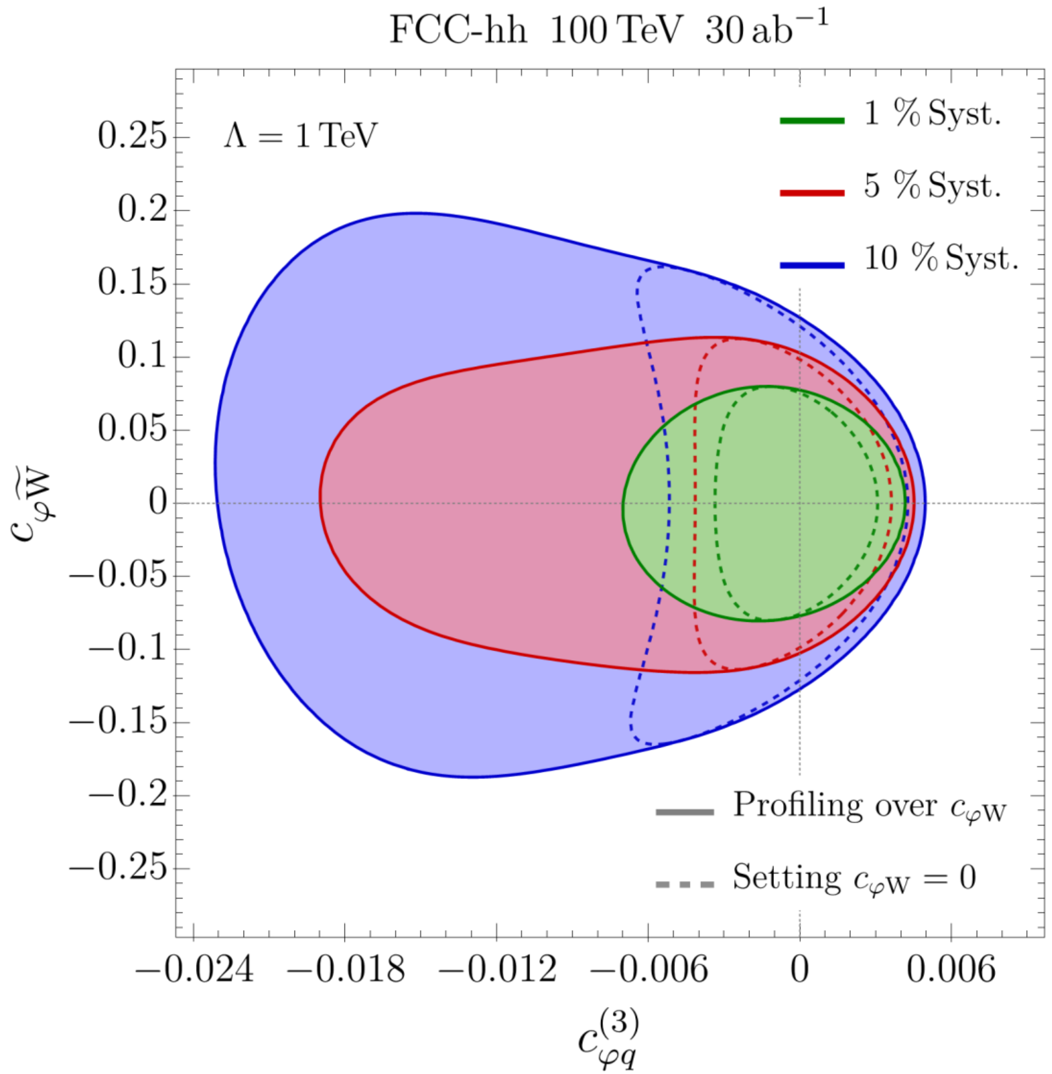

Wh. More results

- 95% CL bounds

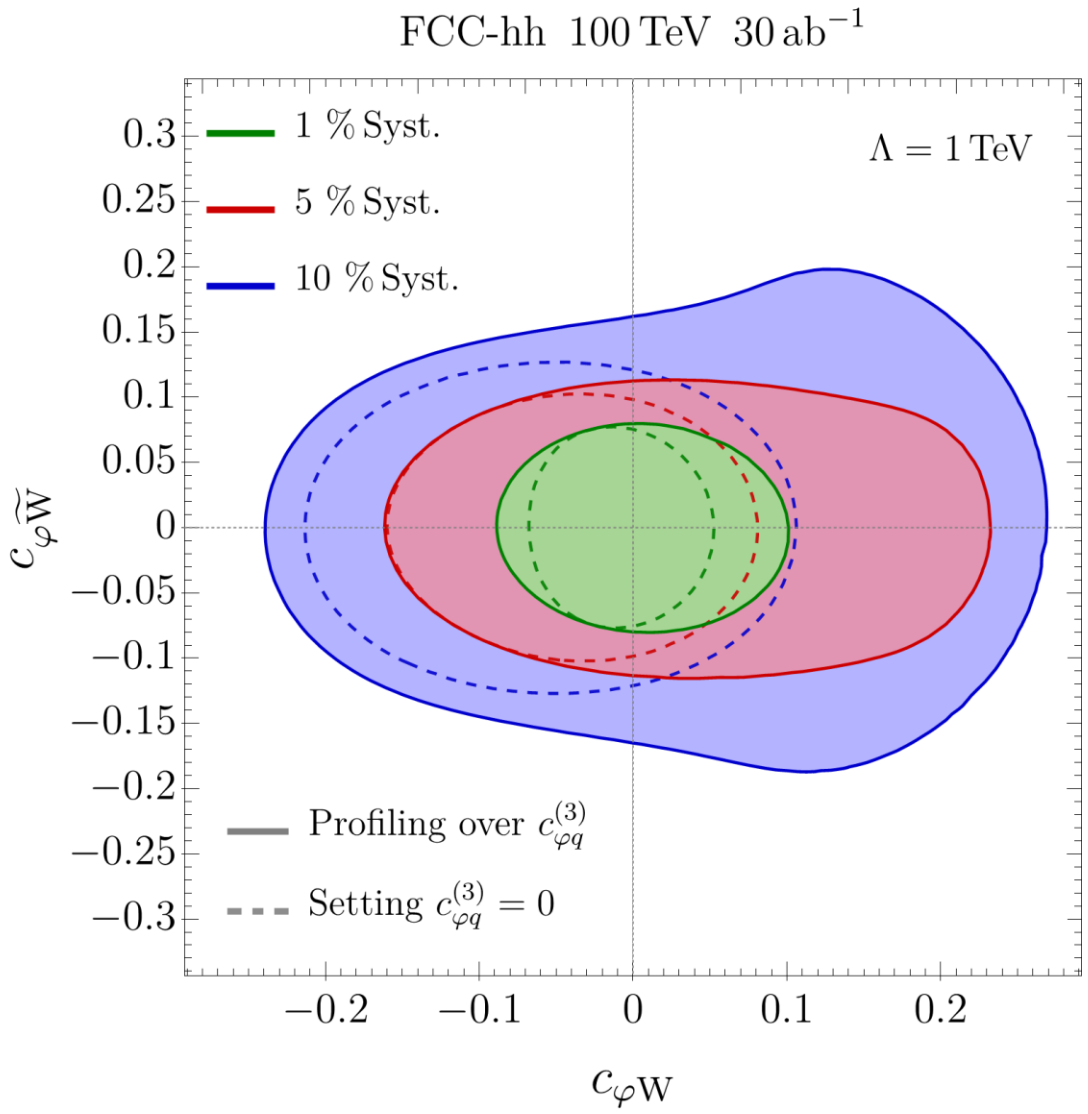

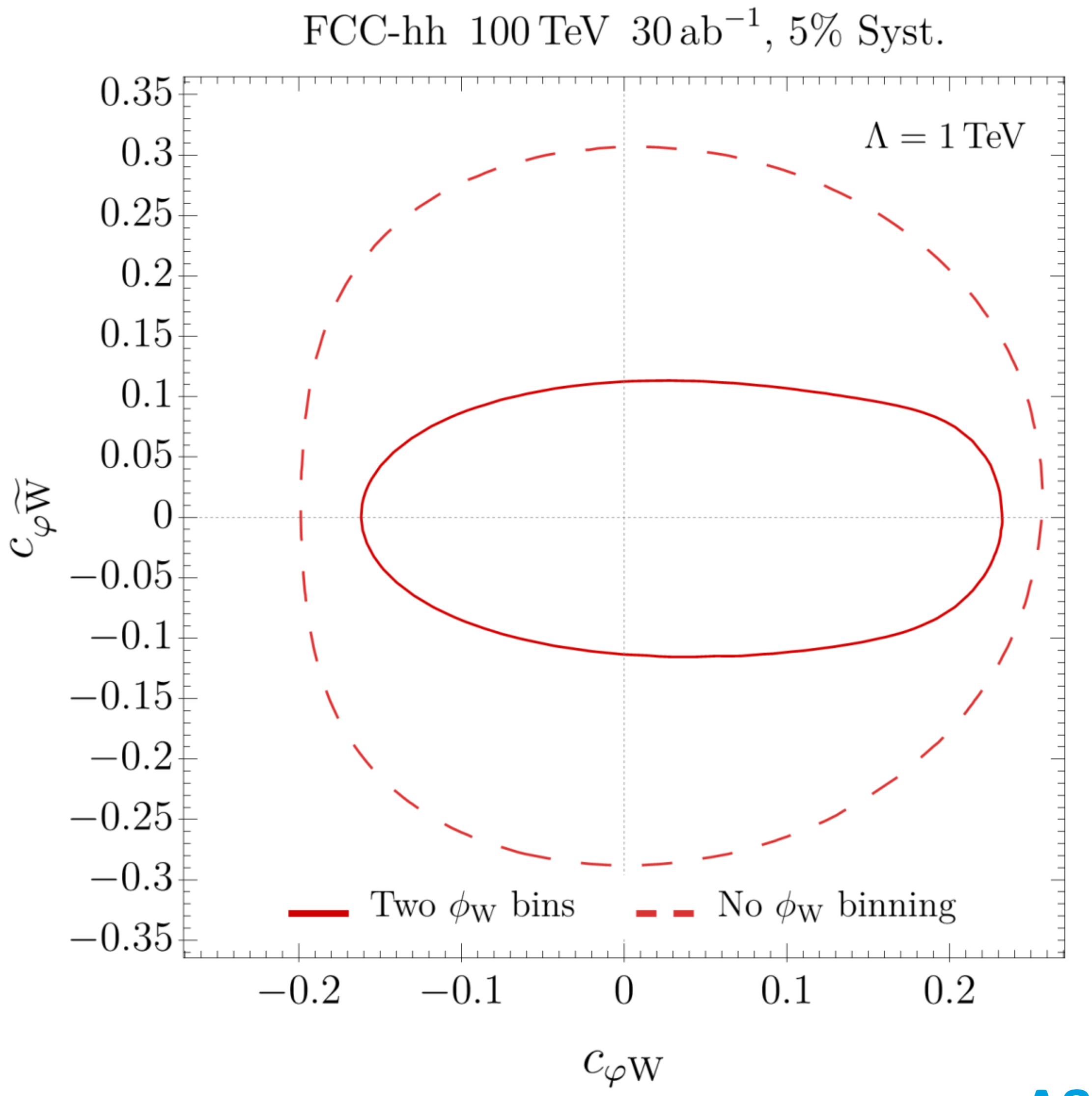

Wh.

More results

- 95% CL bounds summary

Coefficient	Profiled Fit		One Operator Fit	
$c_{\varphi q}^{(3)}$	$[-5.1,\ 3.4] \times 10^{-3}$	1% syst.	$[-2.7,\ 2.5] \times 10^{-3}$	1% syst.
	$[-11.6,\ 3.8] \times 10^{-3}$	5% syst.	$[-3.3,\ 2.9] \times 10^{-3}$	5% syst.
	$[-20.6,\ 4.1] \times 10^{-3}$	10% syst.	$[-4.0,\ 3.5] \times 10^{-3}$	10% syst.
$c_{\varphi \mathrm{W}}$	$[-7.1,\ 7.9] \times 10^{-2}$	1% syst.	$[-5.3,\ 4.3] \times 10^{-2}$	1% syst.
	$[-13.0,\ 17.5] \times 10^{-2}$	5% syst.	$[-12.1,\ 6.8] \times 10^{-2}$	5% syst.
	$[-20.0,\ 25.2] \times 10^{-2}$	10% syst.	$[-18.8,\ 9.0] \times 10^{-2}$	10% syst.
$c_{\varphi \widetilde{\mathrm{W}}}$	$[-6.4,\ 6.4] \times 10^{-2}$	1% syst.	$[-6.1,\ 6.1] \times 10^{-2}$	1% syst.
	$[-9.0,\ 8.8] \times 10^{-2}$	5% syst.	$[-8.1,\ 8.1] \times 10^{-2}$	5% syst.
	$[-13.5,\ 14.2] \times 10^{-2}$	10% syst.	$[-10.1,\ 10.1] \times 10^{-2}$	10% syst.

More results

- Bound on aTGCs. $c_{\varphi q}^{(3)}$ is related to aTGCs as follows:

$$c_{\varphi q}^{(3)} = \frac{\Lambda^2}{m_W^2} g^2 (\delta g_L^{Zu} - \delta g_L^{Zd} - c_\theta^2 \, \delta g_{1z})$$

- For theories where the vertex corrections are small (e.g. universal theories), the bound on $c_{\varphi q}^{(3)}$ can be recast as a bound on ∂g_{1z}. For 5% systematics and $\Lambda = 1$ TeV:

	One operator Fit	Profiled global fit
$\partial g_{1z} \in$	$[-5.0, 4.4] \times 10^{-5}$	$[-17.6, 5.8] \times 10^{-5}$

- Bound from other sources:

	LEP ([1902.00134])	Current LHC ([1810.05149])	WZ@HL-LHC ([1712.01310])	FCC-ee ([1907.04311])
$\partial g_{1z} \in$	$[-1.3, 1.8] \times 10^{-1}$	$[-19, 1] \times 10^{-3}$	$[-1, 1] \times 10^{-3}$	$[-5, 5] \times 10^{-4}$

Interference patterns

Helicity amplitudes: High energy behavior

Z polarization	SM	$\mathcal{O}_{\varphi q}^{(3)}$	$\mathcal{O}_{\varphi q}^{(1)}$	$\mathcal{O}_{\varphi u}$	$\mathcal{O}_{\varphi d}$
$\lambda = 0$	1	$\frac{\hat{s}}{\Lambda^2}$	$\frac{\hat{s}}{\Lambda^2}$	$\frac{\hat{s}}{\Lambda^2}$	$\frac{\hat{s}}{\Lambda^2}$
$\lambda = \pm 1$	$\frac{M_Z}{\sqrt{\hat{s}}}$	$\frac{\sqrt{\hat{s}}\, M_Z}{\Lambda^2}$	$\frac{\sqrt{\hat{s}}\, M_Z}{\Lambda^2}$	$\frac{\sqrt{\hat{s}}\, M_Z}{\Lambda^2}$	$\frac{\sqrt{\hat{s}}\, M_Z}{\Lambda^2}$

Zh. Simulation details

- Montecarlo generation: Madgraph5_aMC@NLO v.2.7.3; showering: Pythia 8.2; detector simulation: Delphes v.3.4.1 with FCC-hh card. SMEFT@NLO UFO (http://feynrules.irmp.ucl.ac.be/wiki/SMEFTatNLO)
- Signal simulated at LO and corrected to (QCD+QED) NLO with k-factors. Gluon initiated processes simulated at LO. The rest simulated at QCD NLO.
- Parton level generation cuts:

Cut	Channel $Z \to \nu\bar{\nu}$	Channel $Z \to l^+l^-$
$p^j_{T,\min}$ [GeV]	30	
$p^\gamma_{T,\min}$ [GeV]	50	
$p^l_{T,\min}$	0	30 (only for LO samples)
$\lvert\eta^{\gamma,j}_{max}\rvert$	6.1^1	
$\lvert\eta^l_{max}\rvert$	∞	6.1
$\Delta R^{\ell,\gamma l}$	0.01	
$\Delta R^{\gamma\gamma}$	0.25 (0.01 for LO samples)	
$p_T^{V,j}$	$\{0, 200, 400, 600, 800, 1200, \infty\}$	

Zh. Analysis details

- Selection cuts and binning:

$Z \to \nu\bar{\nu}$		$Z \to l^- l^+$
Bins of $\lvert y^h \rvert$	Bins of $min\{p_T^h, p_T^Z\}$	Bins of $\lvert y^{Zh} \rvert$
[0, 2), [2, 6]	[200, 400)	[0, 2), [2, 6]
	[400, 600)	
[0, 1.5), [1.5, 6]	[600, 800)	
[0, 1), [1, 6]	[800, 1000)	
	[1000, ∞)	

	Selection cuts
$p_{T,\min}^{\ell}$ [GeV]	30
$p_{T,\min}^{\gamma}$ [GeV]	50
$m_{\gamma\gamma}$ [GeV]	[120, 130]
$m_{l^+l^-}$ [GeV]	[81, 101]
$\Delta R_{\max}^{\gamma\gamma}$	$\{1.3, 0.9, 0.75, 0.6, 0.6\}$
$\Delta R_{\max}^{l^+l^-}$	$\{1.2, 0.8, 0.6, 0.5, 0.4\}$
$p_{T,\max}^{Zh}$ [GeV]	$\{200, 600, 1100, 1500, 1900\}$

- K-factors for signal in 1+QCD+QED format

$p_{T min}$ bin [GeV]	$Zh \to \ell\ell\gamma\gamma$	$Zh \to \nu\nu\gamma\gamma$	$Wh \to \nu\ell\gamma\gamma$
0 – 200	$1 + 0.59 - 0.07 = 1.52$	$1 + 0.26 - 0.06 = 1.20$	$1 + 0.17 - 0.04 = 1.13$
200 – 400	$1 + 0.52 - 0.09 = 1.43$	$1 + 0.31 - 0.09 = 1.22$	$1 + 0.28 - 0.09 = 1.19$
400 – 600	$1 + 0.64 - 0.14 = 1.50$	$1 + 0.37 - 0.14 = 1.23$	$1 + 0.28 - 0.17 = 1.11$
600 – 800	$1 + 0.69 - 0.18 = 1.51$	$1 + 0.40 - 0.18 = 1.22$	$1 + 0.35 - 0.24 = 1.11$
800 – 1000	$1 + 0.70 - 0.24 = 1.46$	$1 + 0.40 - 0.24 = 1.16$	$1 + 0.39 - 0.32 = 1.07$
1000 – ∞	$1 + 0.69 - 0.32 = 1.37$	$1 + 0.40 - 0.32 = 1.08$	$1 + 0.36 - 0.40 = 0.96$

Zh.

More results

- Events per bin for the relevant processes in the neutrino channel. Wh is part of the signal because it is affected by $\mathcal{O}_{\varphi q}^{(3)}$.

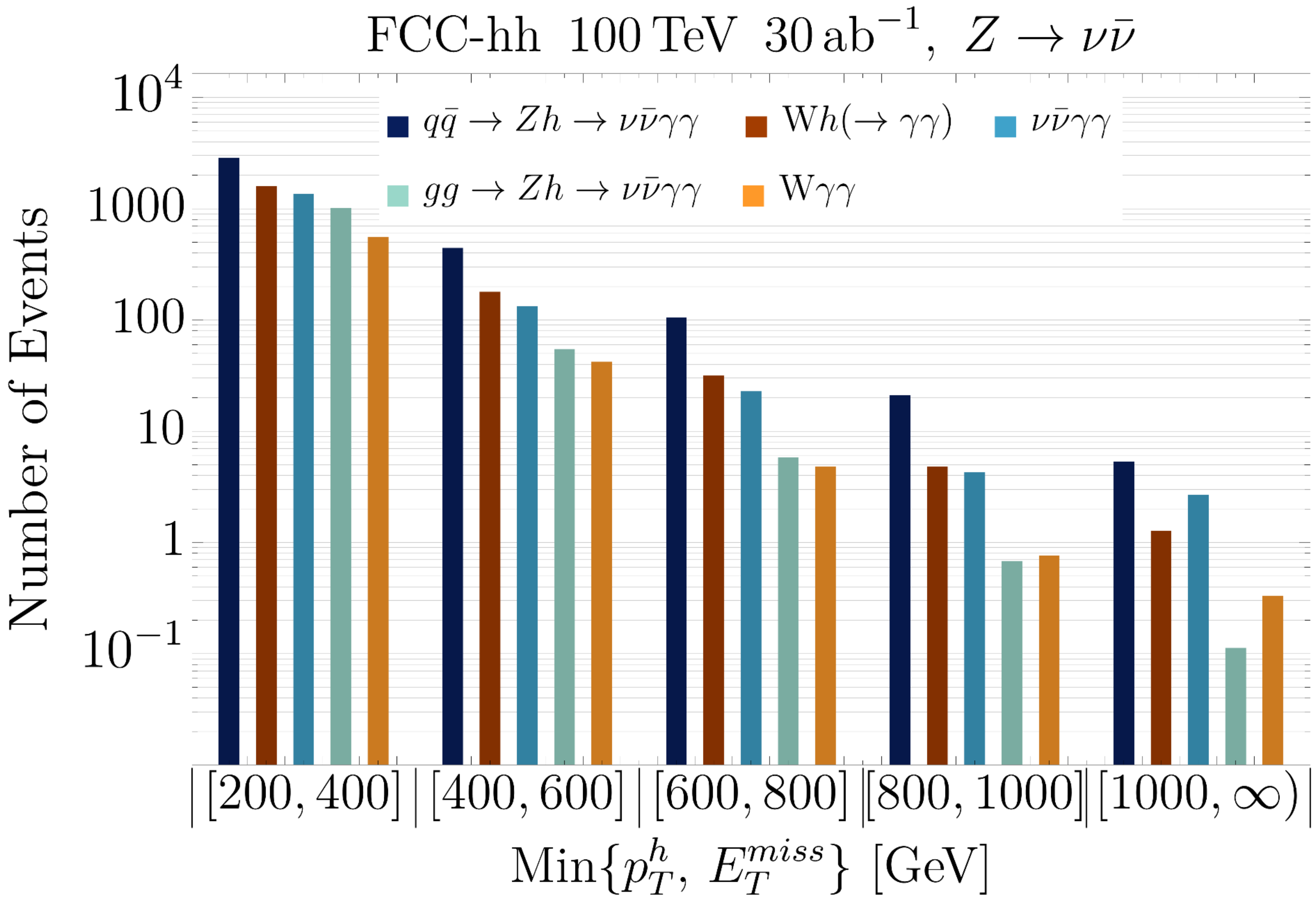

More results

- Events per bin for the relevant processes in the leptonic channel.

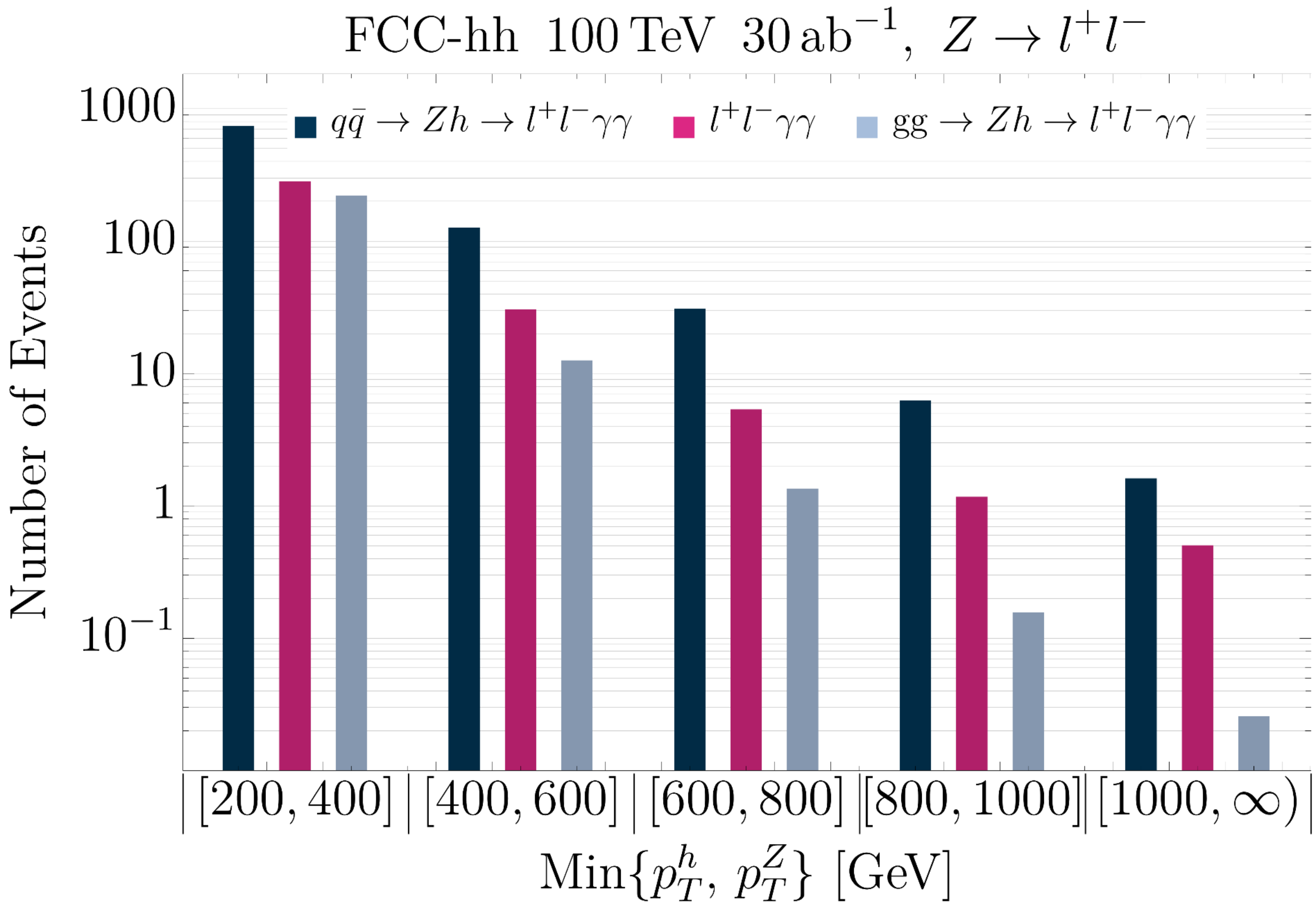

Zh. + Wh. More results

- Bounds on $\mathcal{O}_{\varphi q}^{(3)}$ with one operator fit combiningthe Wh and Zh processes as a function of the NP scale M.

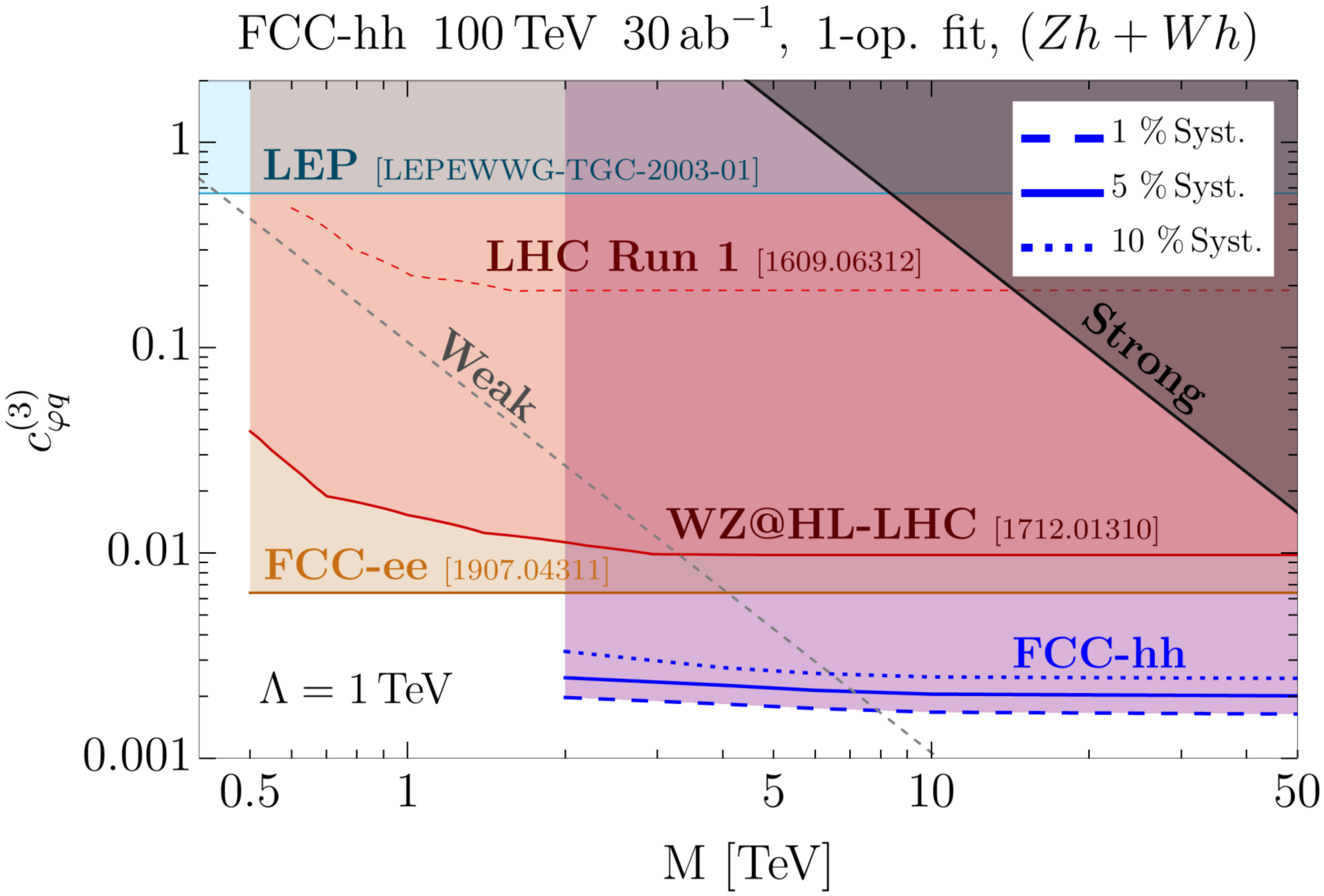

Zh. More results

- 95% CL bounds

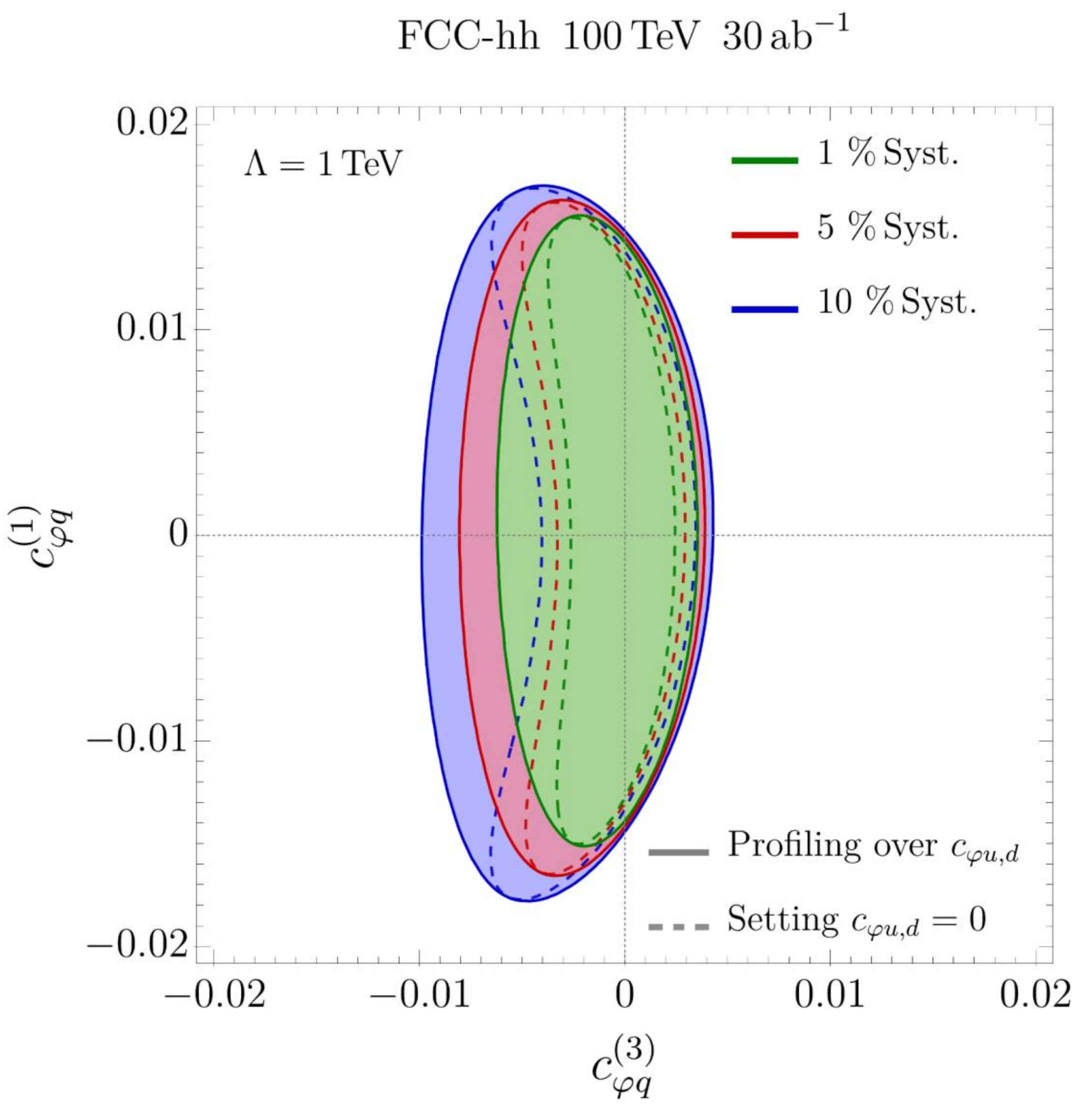

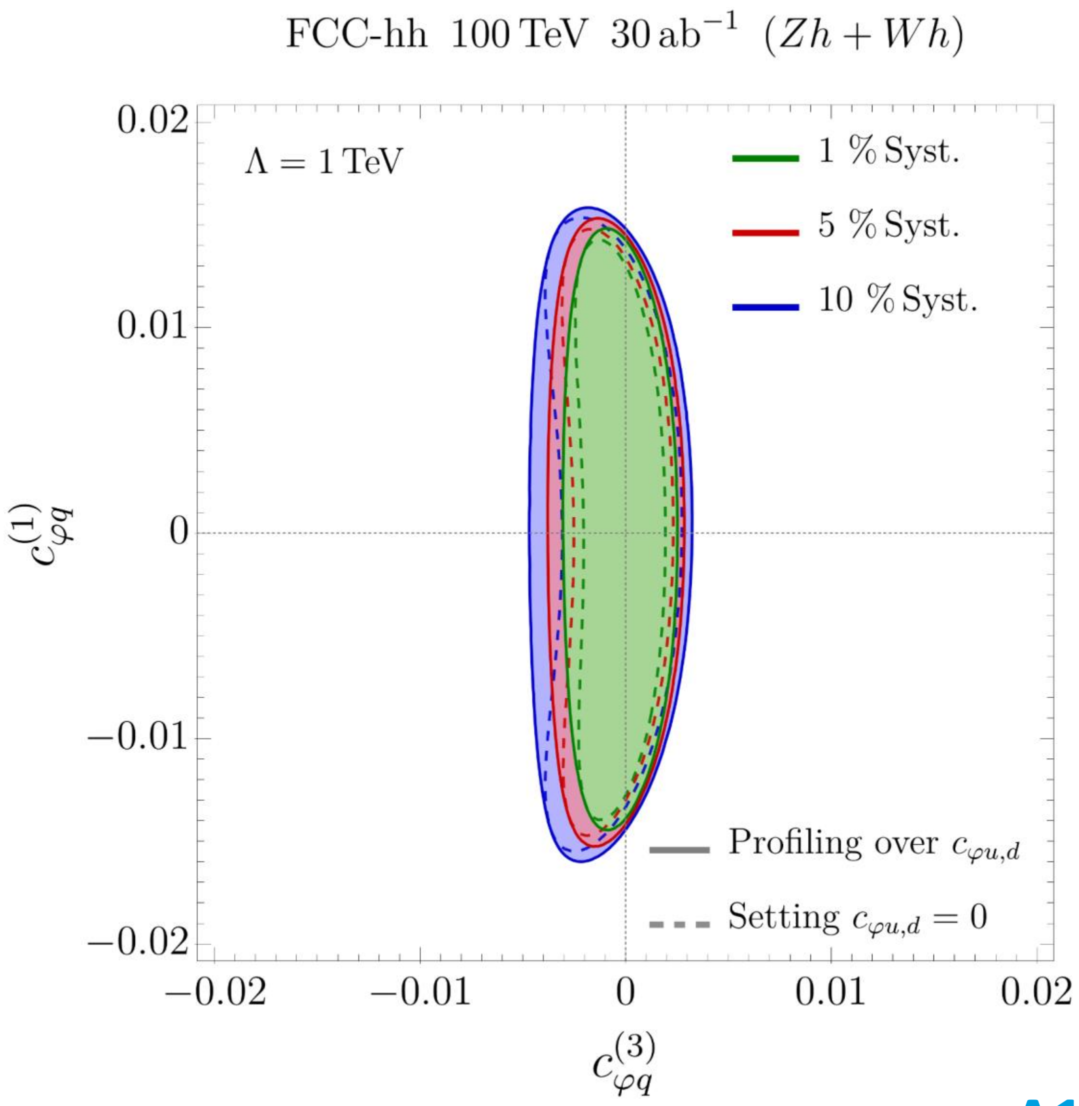

Zh. More results

- 95% CL bounds

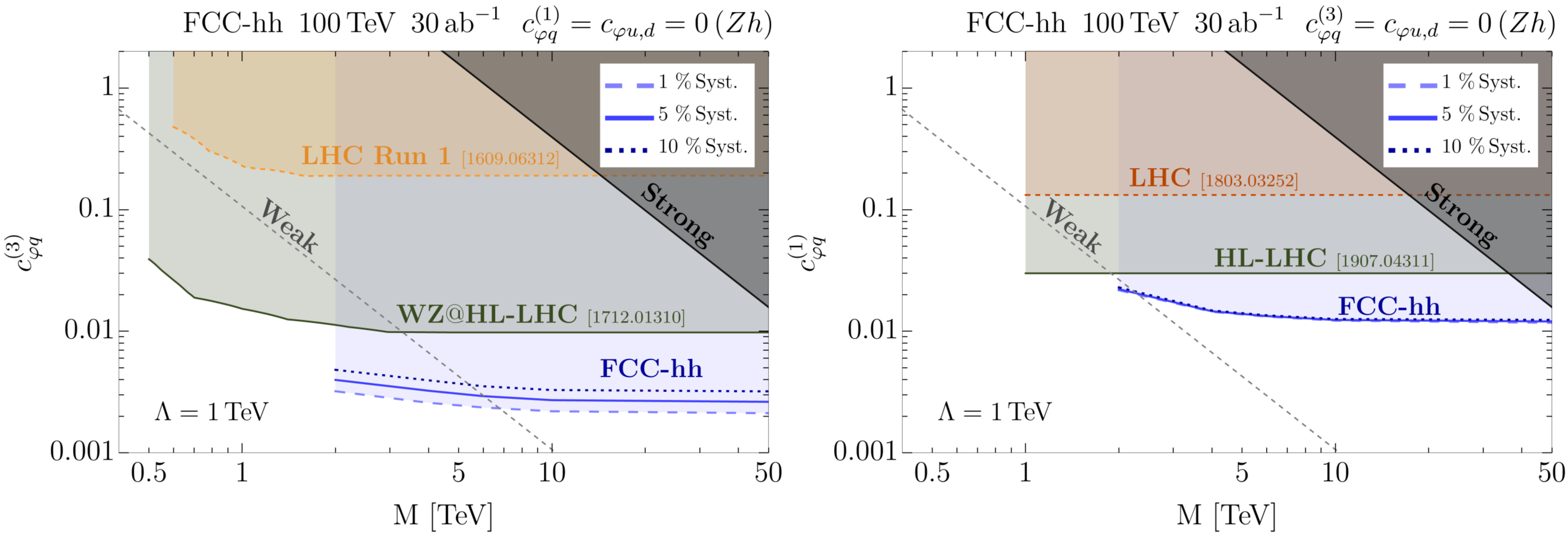

Zh.

More results

- 95% CL bounds summary

Coefficient	Profiled Fit		One Operator Fit	
$c_{\varphi q}^{(3)}$	$[-5.2,\ 3.1] \times 10^{-3}$	1% syst.	$[-2.1,\ 2.0] \times 10^{-3}$	1% syst.
	$[-6.7,\ 3.3] \times 10^{-3}$	5% syst.	$[-2.6,\ 2.4] \times 10^{-3}$	5% syst.
	$[-8.2,\ 3.7] \times 10^{-3}$	10% syst.	$[-3.2,\ 2.8] \times 10^{-3}$	10% syst.
$c_{\varphi q}^{(3)}$ $(+Wh)$	$[-2.5,\ 2.1] \times 10^{-3}$	1% syst.	$[-1.6,\ 1.6] \times 10^{-3}$	1% syst.
	$[-3.0,\ 2.4] \times 10^{-3}$	5% syst.	$[-2.0,\ 1.9] \times 10^{-3}$	5% syst.
	$[-3.7,\ 2.7] \times 10^{-3}$	10% syst.	$[-2.4,\ 2.2] \times 10^{-3}$	10% syst.
$c_{\varphi q}^{(1)}$	$[-1.3,\ 1.4] \times 10^{-2}$	1% syst.	$[-1.1,\ 1.15] \times 10^{-2}$	1% syst.
	$[-1.5,\ 1.5] \times 10^{-2}$	5% syst.	$[-1.1,\ 1.2] \times 10^{-2}$	5% syst.
	$[-1.6,\ 1.5] \times 10^{-2}$	10% syst.	$[-1.2,\ 1.2] \times 10^{-2}$	10% syst.
$c_{\varphi u}$	$[-2.0,\ 1.6] \times 10^{-2}$	1% syst.	$[-1.9,\ 0.89] \times 10^{-2}$	1% syst.
	$[-2.1,\ 1.7] \times 10^{-2}$	5% syst.	$[-2.1,\ 0.96] \times 10^{-2}$	5% syst.
	$[-2.2,\ 1.8] \times 10^{-2}$	10% syst.	$[-2.2,\ 1.0] \times 10^{-2}$	10% syst.
$c_{\varphi d}$	$[-2.1,\ 2.3] \times 10^{-2}$	1% syst.	$[-1.4,\ 2.2] \times 10^{-2}$	1% syst.
	$[-2.2,\ 2.4] \times 10^{-2}$	5% syst.	$[-1.5,\ 2.2] \times 10^{-2}$	5% syst.
	$[-2.3,\ 2.5] \times 10^{-2}$	10% syst.	$[-1.5,\ 2.2] \times 10^{-2}$	10% syst.